

# LIDAR, SUNPHOTOMETER AND SPECTRORADIOMETER MEASUREMENTS OF THE ATMOSPHERIC AEROSOL OPTICAL CHARACTERISTICS

Nikolay Kolev<sup>(1)</sup>, Panuganti Devara<sup>(2)</sup>, Ilko Iliev<sup>(3)</sup>, Tsvetina Evgenieva<sup>(1)</sup>, Boiko Kaprielov<sup>(1)</sup>, Ivan Kolev<sup>(1)</sup>

<sup>(1)</sup> Institute of Electronics, Bulgarian Academy of Sciences, 72, Tsarigradsko shosse Blvd., Sofia 1784, Bulgaria; E-mail: blteam@ie.bas.bg

<sup>(2)</sup> Indian Institute of Tropical Meteorology, Dr. Homi Bhabha Road, NCL Post Office Pashan, PUNE 411 008, India; E-mail: devara@trompet.res.in

<sup>(3)</sup> Central Laboratory of Solar-Terrestrial Influences, Bulgarian Academy of Sciences, E-mail: ilko@stil.acad.bg

## ABSTRACT

This paper presents determination of the optical parameters and the distribution with height of the atmospheric aerosol using three instruments, namely, lidar, sunphotometer and spectroradiometer. A comparison is made between the readings of the three devices, in measuring the aerosol optical depth. The role of the processes in the planetary boundary layer on the atmospheric aerosol optical characteristics is studied.

## 1. INTRODUCTION

In recent years, the comprehensive investigations of the atmospheric aerosol gained new impetus due to the understanding that it plays a substantial role as it influences the climate both on regional and on global scale [1]. Measurements are being carried out by means of active and passive instruments mounted on satellites, airplanes, ships and terrestrial stations. In the past, the lidar measurements of the atmospheric aerosol were aimed mainly at monitoring the atmospheric pollution, or, alternatively, the aerosol was traced in order to follow and study certain atmospheric parameters, such as wind velocity, meteorological visibility, etc. The studies lately were broadened to clarify its influence of the radiative balance of the system sun-atmosphere-earth.

## 2. APPARATUS

We applied well known techniques for processing of lidar and radiometric data [2, 3].

The main parameters of the three devices are:

**Specifications of the lidar** (developed in the Institute of Electronics): **transmitter** – a standard Nd-YAG laser (operational wavelength 532 nm, pulse duration and energy 15–20 ns and 10–15 mJ, repetition rate 12.5 Hz; **receiving antenna** – a Cassegrainian telescope (main mirror diameter 150 mm, equivalent focal length 2250 mm); **photodetector** – a PMT with an interference filter (1 nm FWHM); **data acquisition and processing set** – a 10 bit 20 MHz ADC and a PC. [4]

**Specifications of the sunphotometers Microtops II: optical channels:**  $\lambda=380$  nm,  $\lambda=440$  nm,  $\lambda=500$  nm,  $\lambda=675$  nm,  $\lambda=870$  nm,  $\lambda=936$  nm and  $\lambda=1020$  nm, **viewing angle** –  $2.5^\circ$ , **dynamic range**  $> 3 \times 10^5$ , **computer interface** RS 232, **data storage** – 800 records, **power source** – 4 x AA Alkaline batteries [6].

**Specification of the spectroradiometer** (developed in the Central Laboratory of Solar-Terrestrial Influences): a photographic objective, a prism monochromator, a CCD line (512 pixels), a PMT, a 10 bit ADC, and 8 bit specialized computer (44 kB RAM); **spectrum range** 600–1100 nm, **spectrum resolution** 0.24–5.4 nm, photodetector dynamic range  $10^4$ , time of data accumulation 50 ms–10 s [5].

## 3. EXPERIMENTAL RESULTS AND DISCUSSION

The experiments were carried out in the south-western part of the city of Sofia, where the Institute of Electronics (aerosol lidar) and the Central Laboratory for Solar-Terrestrial Influences (sunphotometer and spectroradiometer) are located. Fig.1 shows the topography of the area (the city of Sofia is located in a mountain valley) and location of the devices.

### 3.1. Lidar, sunphotometer and spectroradiometer data

The lidar data are presented in the form of height-time indicators (HTIs). We used the data to determine the location of the aerosol and the various layers in the cases of stable boundary layer (SBL) and convective boundary layer (CBL). We present data taken on one summer and one autumn day.

In Fig. 2 seven height-time indicators of the lidar signal are shown obtained from 07:10 till 13:10 LST, i.e. during the development of the atmospheric boundary layer (ABL) from SBL to CBL. In the first image the structure of the SBL is well pronounced; several aerosol layers could be clearly seen up to a height of about H=300–400 m, followed by the residual layer (RL) up

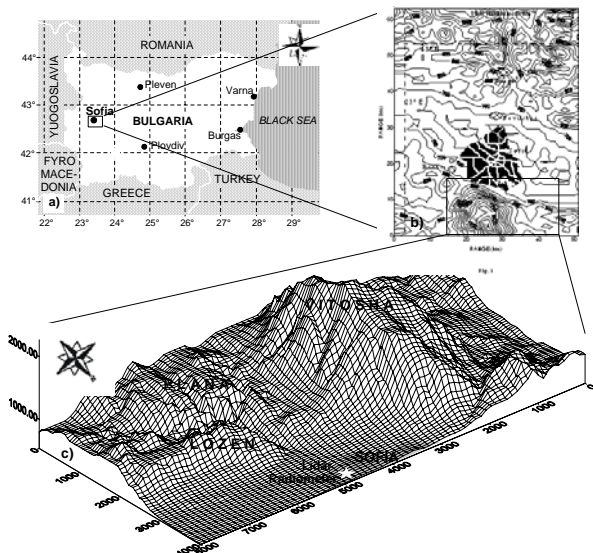


Fig. 1. Location and topography of the experimental site: (a), (b) topographic contours, (c) topography.

to a height of about  $H=700$  (900) m. The destruction of the SBL, formed during the night, starts after 08:10 LST; in the image obtained at 09:10 LST the beginning of the new mixing layer (ML) formation could be clearly distinguished. At 11:15 LST the ML height reached  $H=500$  m and the destruction of the RL started. The height of the ML raised up to  $H=1000-1100$  m till 12:30 LST and up to  $H=1200$  m at 13:10 LST, the latter being not so distinguishable in the figure due to the insufficient print resolution.

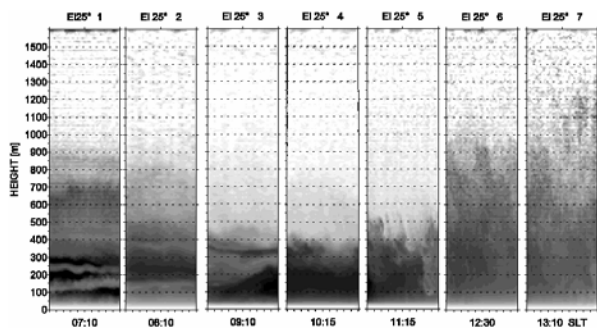


Fig. 2. Height-time indicator constructed on overview from the lidar data obtained on 11.06.2004.

In Fig. 3 contrast with the previous figure, the lidar data do not show the typical aerosol structure above the region in the case of SBL. At 07:30, we observed mainly two layers, which we denoted by RL1 and RL2, the first one extending from height of 100 m to 1000 m, the second, from  $H = 1200$  m to  $H = 1800$  m. The destruction of the first layer began from above at about 09:30 hours; at 10:30 its height was about 700 m; the layer was completely destroyed at approximately 11:00-11:30. The destruction of RL2 began at 09:00;

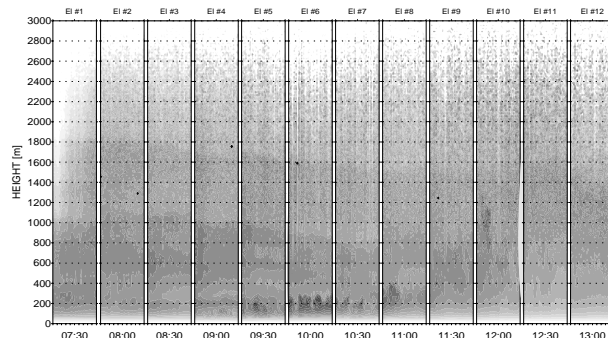


Fig. 3. Height-time indicator constructed on overview from the lidar data obtained on 06.10.2004.

around 11:00-11:30 its height was approximately 1500 m; its destruction was complete about 12:00-12:30.

The new ML began to be formed at 09:00; at 11:00 its height is about 400 m; at 11:30 it is  $H=800-1000$  m; at 12:00 this height is 1300 m; while at 12:30-13:00, the height reaches 1800 m.

Fig. 4 presents aerosol optical depth (AOD) data obtained at six wavelength of the sunphotometer on 07.10.2004. One can clearly see that at, e.g.  $\lambda=500$  nm in the morning hours  $\tau_{as}=0.2$ ; between 10:30 and 12:30,  $\tau_{as}=0.3$ ; and in the afternoon  $\tau_{as}=0.1$ . The AOD is maximal at  $\lambda = 380$  nm and  $\lambda=480$  nm ( $\tau=0.45$ ).

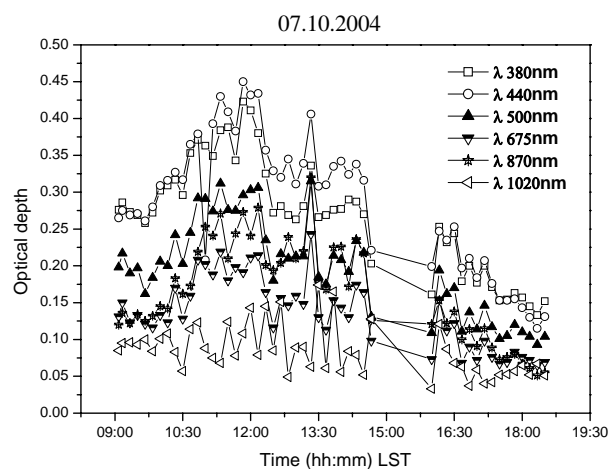


Fig. 4. Aerosol optical depth obtained by the sunphotometer at different wavelengths on 07.10.2004.

The next two figures present spectroradiometer data on the AOD dependence on the wavelength, as well as the AOD variation with the observation time at three wavelengths.

Fig. 5 shows the AOD spectral behavior with the wavelength varying from  $\lambda=540$  nm to  $\lambda=680$  nm at three different moments of observation. It is seen that

during the measurement period the spectral optical depth does not vary significantly; however, two local maxima can be clearly seen around  $\lambda = 600$  nm and  $\lambda = 660$  nm. It is also seen that the spectral AOD at 16:30 h exceeds the one measured at 15:20 h.

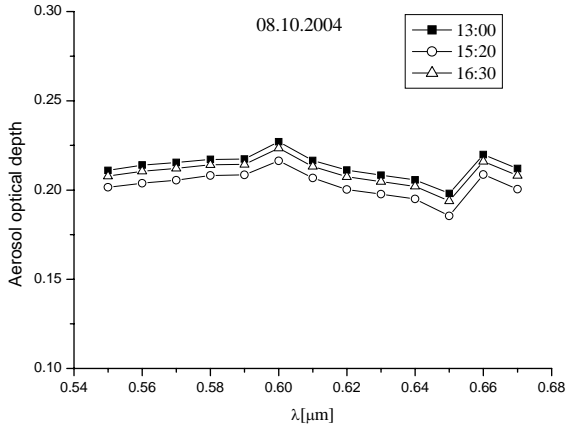


Fig. 5. Aerosol optical depth obtained by the spectro-radiometer at different wavelengths on 08.10.2004.

Fig. 6 shows AOD data taken at three close wavelengths, namely,  $\lambda=550$  nm,  $\lambda=600$  nm, and  $\lambda=650$  nm, as well as their temporal behavior. The AOD values remain close and almost constant, in the range  $\tau_{ar}=0.2-0.25$ . We should note here that the AOD values at  $\lambda = 600$  nm are the largest during the measurements. In conclusion, let us remark that on both dependencies (Fig. 5 and Fig. 6) the AOD values are the largest at  $\lambda=600$  nm.

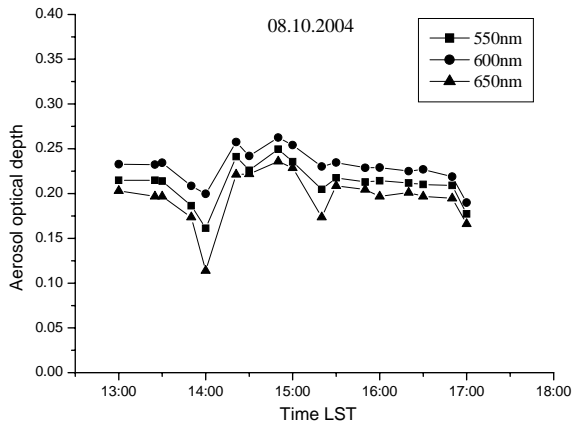


Fig. 6. Variatiron of aerosol optical depth obtained by the spectroradiometer on 08.10.2004.

### 3.2. Analysis of the data obtained

The data analysis was performed by first considering jointly the lidar and the sunphotometer data. The lidar data formed the basis of this analysis, since they had

been accumulated for this region for many years.

Fig. 7 shows the RL, ML, and AOD variation as determined from the lidar data (the extinction coefficient was calculated using the Klett technique [7] and the sunphotometer data taken on 07.10.2004. One can distinctly see that according to the sunphotometer data the AOD reaches its maximal value  $\tau_{as}=0.3$  at  $\lambda=500$  nm before the ML reaches its maximal height of 900 m at 14:00 LST; the AOD determined from the lidar data varies smoothly from  $\tau_{al}=0.1$  after the SBL destruction, reaches  $\tau_{al}=0.2$  after the ML formation, and remains almost constant afterwards.

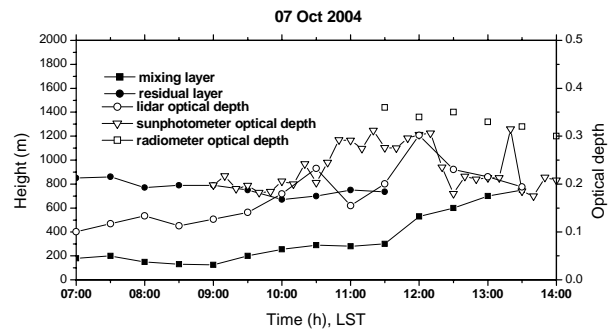


Fig. 7. Variation in the heights of residual layer, stable layer, mixing layer and in the aerosol optical depth on 07.10.2004.

Based on the sunphotometer data shown in Fig. 4, bearing in mind in particular the well expressed maxima at the shorter wavelengths ( $\lambda=380$  nm and  $\lambda=480$  nm), one can assume that the aerosol particles affecting substantially the AOD are of the sub-micron fraction ( $d=0.3-1.0$   $\mu\text{m}$ ).

The lidar signal in Fig. 3 demonstrates that the backscattering coefficient is the largest from 09:30 to 12:00; it decreases afterwards and remains constant between 12:30 and 13:30, when the ML has already been fully formed. At 10:30 the SBL has been destroyed, while the ML reaches the RL and starts to destroy it from below. According to the lidar data, the AOD rises most significantly from 10:30 till 12:10 (from  $\tau_{al}=0.1$  to  $\tau_{al}=0.2$ ), which better expressed in the sunphotometer data, as we mentioned above. Since in this period the new ML destroys completely the RL, one can assume that the so-called entrainment process takes place, i.e., mixing from above of dry aerosol from the ML with wet aerosol from the ML. The AOD exhibits also a similar behavior on 08.10.2004. On 05.10 and 06.10.2004, the sunphotometer data yield AOD varying around  $\tau_{as}=0.2$ . The lidar data for this case indicate that the RL from the previous day and newly formed ML reach maximal heights of  $H=1800-2000$  m which evidences that the synoptical situation is not affected by the local phenomena taking place in the region.

Fig. 8 presents the AOD data taken on 08.10.2004 by means of the three devices, namely, a lidar, a sunphotometer and a spectroradiometer. As one can clearly see again, the AOD determined by the two passive devices exceeds the values obtained by using the lidar data. This holds true for all measurements, since the lidar measures the AOD within the lidar range, namely, in the planetary boundary layer (PBL), while the photometer and radiometer measures the AOD along the entire path between the Sun and the Earth [8]. The data were acquired in the afternoon hours only, but agree well with and complement the sunphotometer data.

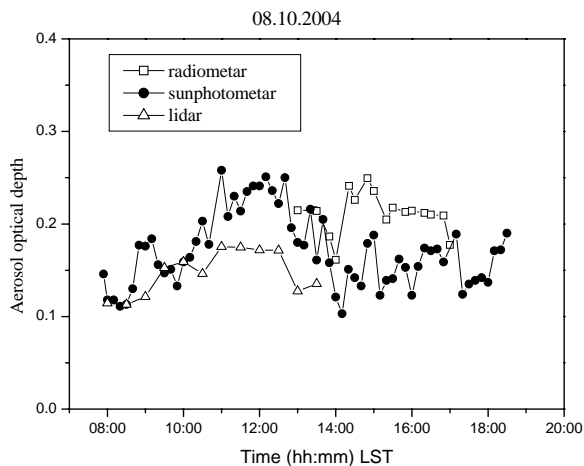


Fig. 8. Variation in the aerosol optical depth obtained on 08.10.2004

Our next step was to determine the Angstrom  $\alpha$  and  $\beta$  [9] which are presented on Fig. 9. The data on  $\beta$  for all measurements point to a medium atmospheric turbidity.

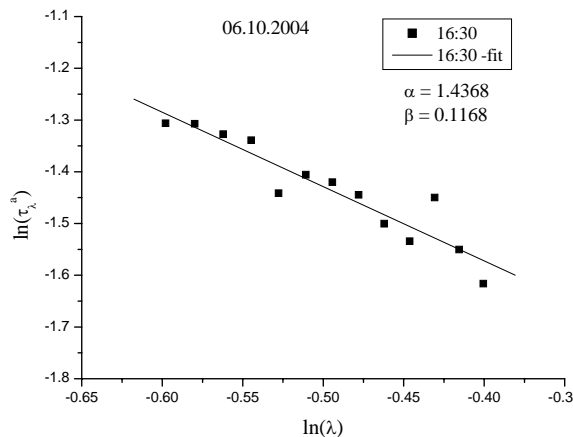


Fig. 9 Determination of the Angstrom coefficients on 06.10.2004.

#### 4. CONCLUSIONS

The optical characteristics of the atmospheric aerosol are studied using active and passive remote means.

It could be definitely concluded that the combined study of the atmospheric aerosol over an urban area situated in a mountain valley by means of the remote sensing, on one hand, improves our knowledge concerning its optical properties (AOD and Angstrom parameters) and, on the other, gives a possibility of studying the role of the processes taking place in the PBL in their interaction with manifestation of the different forms of the mountain-valley circulation on the atmospheric aerosol.

At the same time the present study allows a set of ground based instruments to be tested, which could be successfully used in combination with satellite-based equipment for global investigation of the atmosphere as reference points in different regions along the satellites' trajectories.

#### 5. REFERENCES

1. Kanfman Y. J., et al., A satellite view of aerosols in the climate system, *Rev. Nature*, Vol. 419, 215-223, 2002.
2. Menut L., et al. Urban boundary layer height determination from lidar measurements over the Paris area. *Applied Optics*, Vol. 36, 357-375, 1999.
3. Devara P.C.S., et al. Investigation of aerosol optical depth variations using spectroradiometer at an urban station, Pune, India, *J. Aerosol Sci.*, Vol. 27, No. 4, 621-632, 1996.
4. Kolev I. et. al.. Lidar observation of the nocturnal boundary layer formation over Sofia, Bulgaria, *Atmospheric Environment*, Vol. 34, 3223-3235, 2000.
5. Mishev D. N., and Iliev I.. System for measuring and registration of the structure of the solar irradiance spectrum, *Compt. Rend. Acad. Bul. Sci*, Tome 45, No. 12, 41-44, 1992.
6. Kolev N., et al.. Lidar-solar radiometer characterization of urban boundary layer over Sofia, Bulgaria: preliminary results. *Abstracts of 5th UAQ, Valencia, Spain 29-31 March*, 84, 2005.
7. Klett J. D. Stable analytical inversion solution for processing lidar return signal, *Appl. Opt.*, Vol. 20, 211-220, 1981.
8. Takamura T., et al.. Tropospheric aerosol optical properties derived from lidar, sunphotometer and optical particle counter measurements, *Applied Optics*, Vol. 33, 7132-7140, 1994.
9. Cachorro V. E., et al. Determination of the Angstrom turbidity parameters, *Applied Optics*, Vol. 26, 3069-3076, 1987.